

A Comparative study on Ferro-fluid Lubricated Porous Journal Bearing

Dipak A Patel^{1*}, Manisha Joshi², Dilip B. Patel³

¹Humanities and Sciences Department, Government Engineering College Palanpur – 385001, Gujarat State, India.

Email id: da.ab44@gmail.com

²Dean, Undergraduate Program, IILM University, Gurugram – 122003, Haryana, India.

Email id: manishajos@yahoo.co.in

³College of Renewable Energy and Environmental Engineering, S. D. Agricultural University, Sardarkrushinagar – 385506, Gujarat State, India

Email id: dilipkumar15781@gmail.com

Abstract: This research considered hydrodynamic theory on ferro-fluid flow models such as R. E. Rosensweig model and Jenkins model for axially undefined journal bearing with porous attached at the inner surface (i.e. on the journal). In this study, the variable external magnetic field is assumed. The expressions of (non-dimensional) pressure and load-carrying capacity are obtained. The values of load capacity for both models are calculated for various parameters like porous thickness, slip velocity, squeeze velocity, permeability, and eccentricity. Also, calculated load capacity by considering porous structure models like the globular sphere model and capillary fissures model. Based on the obtained results, the globular sphere model gives much better performance for load capacity rather than the capillary fissures model. From the study, it is suggested that to design the journal bearing, globular sphere model of porous structure should be preferred over the capillary fissures model. Also, for the better performance of the journal bearing, the choice of fluid-flow model depends on the values of parameters.

Keywords: Magnetic Fluid, Journal Bearing, Neuringer-Rosensweig Model, Jenkins Model.

(Article history: Received: 17th May 2021 and accepted 27th June 2022)

I. INTRODUCTION

In machine mechanism point of view, where vibrations are there like engines of motor vehicles, turbines, printers, gear, pumps, etc., hydrodynamic journal bearings are broadly used. In all such types of machinery, there is a circular shaft (inner solid reference of bearing) known as a journal (shaft) sometimes called a shafting, which rotates inside a circular outer. It is notable that most journal bearings have common applications that use a lubricant fluid to diminish the friction between the moving surfaces. During the operational mode, smooth conduction of bearing and proper lubrication is required for the bearing. This improves the life of bearings and enhances the performance.

The magnetic fluid is made with fine iron-oxide particles covered with surfactant and added to the base fluid. These fluids can be placed, designed, and controlled at a specific location that prompts the use of magnetic fluid in the lubrication of bearings. Many authors [3-9] have considered magnetic fluid as a lubricant in their research on bearing problems.

Neuringer and Rosensweig [3] have given a straightforward model to explain the flow of magnetic fluids in the occurrence of fluctuating external magnetic fields in 1964. By considering various types of bearings, many authors have done a good amount of research by considering Neuringer-Rosensweig model (NR Model). In view of Maugin's [1] modifications, Jenkins [4] modified the NR model flow model in 1972. It was concluded that the Jenkins model (JE Model) modifies fluid velocity and pressure both whereas NR model modifies pressure only. Using JE Model,

Ram and Verma [7] studied a porous inclined slider bearing and generalized the analysis done by Agrawal [9] in the case of the NR model.

Up to this, no one has taken the slip condition into consideration. Beavers and Joseph [11] and Sparrow [21] found that such a condition was false at the minimal edge of porous material. Prakash and Vij [10] analyzed the performance of journal bearings, and their analysis considered the velocity slip at the surface of the porous medium with Beavers and Joseph [11] criterion.

Many authors [16-18] have done their studies on magnetic fluid lubricated journal bearing problems, but none of the authors has attached the porous layer on the journal (shaft) which means the inner surface of the bearing.

The aim of the study is to carry out the comparison between the NR Model and the JE Model in the case of axially undefined journal bearing by using a magnetic fluid as a lubricant. The expressions of pressure and load-carrying capacity are obtained for axially undefined journal bearing by using a magnetic fluid as a lubricant in which various parameters have been studied and concluded which model is more suitable in such cases. Also, various porous structure models such as a globular sphere model [19] (introduced by Kozeny-Carman) and a capillary fissures model [20] (Irmay) are taken in to consideration for the study. The Reynolds's type equation is derived. For the Bearing under study, dimensionless load-carrying capacity is calculated for its extreme performance.

II. FLOW MODELS FOR MAGNETIC FLUIDS

Neuringer and Rosensweig [3] have given a straightforward model to explain the flow of magnetic fluids in the existence of changing external magnetic fields in 1964. The basic flow equations of NR Model [3] are:

$$\rho[\bar{q} \cdot \nabla] \bar{q} = -\nabla p + \eta \nabla^2 \bar{q} + \mu_0 (\bar{M} \cdot \nabla) \bar{H}, \quad (1)$$

$$\nabla \cdot \bar{q} = 0, \quad (2)$$

$$\nabla \times \bar{H} = 0, \quad (3)$$

$$\nabla \cdot (\bar{H} + \bar{M}) = 0, \quad (4)$$

$$\bar{M} = \bar{\mu} \bar{H}, \quad (5)$$

where ρ is the density of fluid, \bar{q} is the fluid velocity vector in film region, p is film pressure, η is viscosity of fluid, μ_0 is free space permeability, \bar{M} is the magnetization vector, \bar{H} is the applied magnetic field, $\bar{\mu}$ is magnetic susceptibility of the fluid. In 1972, Jenkins modified the NR flow Model and presented the term which depends on material parameter α^2 (the SI unit of α^2 is $m^3 s^{-1} A^{-1}$) and gave rise to a force $\left(-\frac{\rho \alpha^2 \bar{\mu}}{2} \frac{\partial}{\partial z} \left(H \frac{\partial u}{\partial z} \right), 0, \frac{\rho \alpha^2 \bar{\mu}}{2} \frac{\partial}{\partial x} \left(H \frac{\partial u}{\partial z} \right) \right)$, (6)

in the domain $0 \leq x \leq 2\pi$ (i.e., in the film region.), where H is magnitude of \bar{H} and u is fluid velocity component of \bar{q} in the directions of x -direction.

Due to the force as in (6), the modified NR Model is known as JE Model and flow equations (1), (4) and (5) becomes (Jenkins [4] and Ram and Verma [7]):

$$\rho[\bar{q} \cdot \nabla] \bar{q} = -\nabla p + \eta \nabla^2 \bar{q} + \mu_0 (\bar{M} \cdot \nabla) \bar{H} + \rho \alpha^2 \nabla \times \left(\frac{\bar{M}}{M} \times \bar{M}^* \right), \quad (7)$$

$$\nabla \cdot (\bar{H} + 4\pi \bar{M}) = 0, \quad (8)$$

$$\bar{M} = \bar{\mu} \bar{H}, \quad (9)$$

and

$$\bar{M}^* = \frac{1}{2} (\nabla \times \bar{q}) \times \bar{M}, \quad (10)$$

III. ANALYSIS

There are various types of journal bearings used in machines. One of the types of such bearing system shown in Fig. 1. The cross-segment of Fig. 1 is presented in Fig. 2, which is the configurations of journal bearing taken for this study. It is considered that R is the radius of journal, l is uniform thickness of attached porous layer with journal. Choose the geometry by taking origin O as shown in Fig. 2, the x -axis along with circumference and z -axis is perpendicular to it. The slip velocity s is generated between film region and porous layer. Also \dot{h} is squeeze velocity which is generated during the operating mode (i.e., when outer surface approaches to the journal). Fig. 3 shows the bearing is opened up at the origin O as shown in Fig. 2. The journal circumference is on the θ -axis which lies on $[0, 2\pi]$.

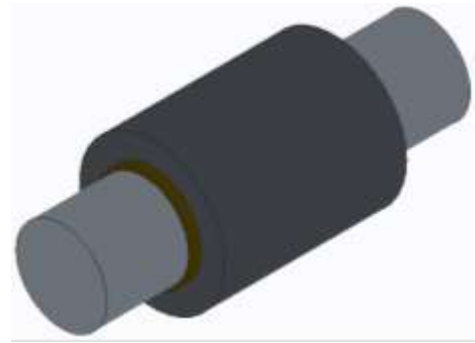


Fig. 1. Journal Bearing

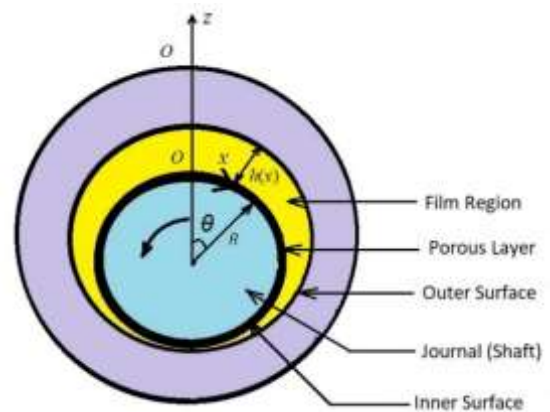


Fig. 2. Configurations of journal bearing

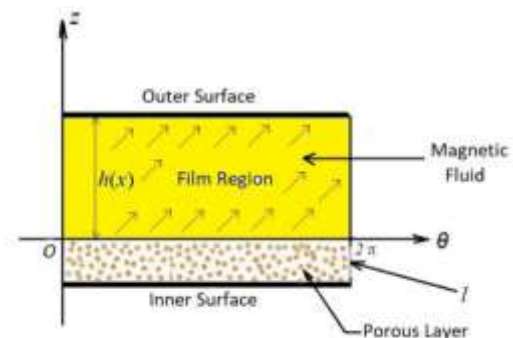


Fig. 3. Journal bearing opened up at O Making use of the conventions of hydrodynamic lubrication and the flow is steady and axially symmetric, (2), (3), (7)-(10) take the form

$$\frac{\partial^2 u}{\partial z^2} = \frac{1}{\eta \left(1 - \frac{\rho \alpha^2 \bar{\mu} H}{2\eta} \right)} \frac{d}{dx} \left(p - \frac{1}{2} \mu_0 \bar{\mu} H^2 \right), \quad (11)$$

where expression of H is

$$H^2 = Kx(2\pi R - x), \quad (12)$$

where K is a quantity such that the dimensions of (12) and the field strength. φ_x and η_x denotes the permeability in

lower porous matrix in x -direction and the porosity of the lower porous region in x -direction respectively. Solving (11) under the boundary conditions [8]

$$u = \frac{1}{s} \frac{\partial u}{\partial z}, \text{ when } z = 0$$

and

$$u = 0, \text{ when } z = h,$$

where h is film thickness, s is a slip defined by $\frac{1}{s} = \frac{\sqrt{\varphi_x \eta x}}{5}$, one obtains

$$u = \frac{(1+hs)z^2 - szh^2 - h^2}{2\eta(1+hs)\left(1 - \frac{\rho\alpha^2\bar{\mu}H}{2\eta}\right)} \frac{\partial}{\partial x} \left(p - \frac{1}{2}\mu_0\bar{\mu}H^2 \right) \quad (13)$$

The velocity components of the fluid in the porous region in x -direction and z -direction are

$$\bar{u} = -\frac{\varphi_x}{\eta} \left[\frac{\partial}{\partial x} \left(p - \frac{1}{2}\mu_0\bar{\mu}H^2 \right) + \frac{\rho\alpha^2\bar{\mu}}{2} \frac{\partial}{\partial z} \left(H \frac{\partial u}{\partial z} \right) \right] \quad (14)$$

and

$$\bar{w} = -\frac{\varphi_z}{\eta} \left[\frac{\partial}{\partial z} \left(p - \frac{1}{2}\mu_0\bar{\mu}H^2 \right) - \frac{\rho\alpha^2\bar{\mu}}{2} \frac{\partial}{\partial x} \left(H \frac{\partial u}{\partial z} \right) \right] \quad (15)$$

respectively. In (14) and (15), P denotes fluid pressure in both the porous region and in (15), φ_z represents permeability in lower porous matrix in z -direction. Now the continuity equation in porous matrix is

$$\frac{\partial \bar{u}}{\partial x} + \frac{\partial \bar{w}}{\partial z} = 0. \quad (16)$$

By using (14)-(15) and integrating (16) with respect to z over $(-l, 0)$ yields

$$\varphi_x l \frac{\partial^2}{\partial x^2} \left(p - \frac{1}{2}\mu_0\bar{\mu}H^2 \right) + \varphi_z \frac{\partial}{\partial z} \left(p - \frac{1}{2}\mu_0\bar{\mu}H^2 \right) \Big|_{z=0} + (\varphi_x - \varphi_z) \frac{\rho\alpha^2\bar{\mu}}{2} \frac{\partial}{\partial x} \left(H \frac{\partial u}{\partial z} \right) \Big|_{z=-l} = 0 \quad (17)$$

by Morgan-Cameron approximation [10] and the surface is solid at $z = -l$. Equation (17) is equivalent to

$$\begin{aligned} & \frac{\partial}{\partial z} \left(p - \frac{1}{2}\mu_0\bar{\mu}H^2 \right) \Big|_{z=0} \\ &= -\frac{\varphi_x l}{\varphi_z} \frac{\partial^2}{\partial x^2} \left(p - \frac{1}{2}\mu_0\bar{\mu}H^2 \right) \\ & \quad - \frac{(\varphi_x - \varphi_z)\rho\alpha^2\bar{\mu}}{2\varphi_z} \frac{\partial}{\partial x} \left(H \frac{\partial u}{\partial z} \right) \Big|_{z=-l} \end{aligned} \quad (18)$$

The film thickness is $h = c(1 + \varepsilon \cos\theta)$, where ε and c being the eccentricity ratio and the radial clearance respectively. The derivative of h with respect to time t is known as squeeze velocity and is $\dot{h} = c\dot{\varepsilon} \cos\theta$, where $\dot{\varepsilon} = \frac{d\varepsilon}{dt}$. As the fluid velocity components are continuous across the surface $z = 0$, $w|_{z=0} = \dot{h} - \bar{w}|_{z=0}$.

Hence

$$\begin{aligned} & w|_{z=0} \\ &= \dot{h} + \frac{\varphi_z}{\eta} \frac{\partial}{\partial z} \left(p - \frac{1}{2}\mu_0\bar{\mu}H^2 \right) \Big|_{z=0} \\ & \quad - \frac{\varphi_z \rho \alpha^2 \bar{\mu}}{2\eta} \frac{\partial}{\partial x} \left(\frac{-sh^2 H}{2\eta(1+hs)\left(1 - \frac{\rho\alpha^2\bar{\mu}H}{2\eta}\right)} \frac{\partial}{\partial x} \left(p - \frac{1}{2}\mu_0\bar{\mu}H^2 \right) \right) \end{aligned} \quad (19)$$

The integral form of continuity equation over the film region $(0, h)$ is

$$\frac{\partial}{\partial x} \int_0^h u dz + w_h - w_0 = 0. \quad (20)$$

Here $w_h = 0$ due to solid surface at $z = h$. Therefore (20) rewrites as

$$\frac{\partial}{\partial x} \int_0^h u dz = w_0 \quad (21)$$

Substituting the expressions as in (13) and (19) in (21), one obtains the Reynold's Type equation as

$$\frac{d}{d\theta} \left[g \frac{d}{d\theta} \left(p - \frac{1}{2}\mu_0\bar{\mu}H^2 \right) \right] = -12\eta R^2 c \dot{\varepsilon} \cos\theta, \quad (22)$$

using $x = R\theta$, where

$$g = -12\varphi_x l + \frac{(4+hs)h^3 + \left(3s\rho\alpha^2\bar{\mu}\varphi_z h^2 H / \eta\right)}{(1+hs)\left(1 - \frac{\rho\alpha^2\bar{\mu}H}{2\eta}\right)} - \frac{6\rho\alpha^2\bar{\mu}(\varphi_x - \varphi_z)lh}{\eta\left(1 - \frac{\rho\alpha^2\bar{\mu}H}{2\eta}\right)}$$

Using the dimension less quantities

$$\psi_x = -\frac{\varphi_x l}{c^3}, \quad \bar{s} = sc, \quad \beta = \frac{\rho\alpha^2\bar{\mu}\sqrt{KR}}{2\eta}, \quad \gamma^* = \frac{6\varphi_z}{c^2},$$

$$\psi_z = \frac{\varphi_z l}{c^3}, \quad \bar{h} = \frac{h}{c}, \quad \mu^* = \frac{K\mu_0\bar{\mu}c^2}{2\eta\varepsilon}, \quad \bar{p} = \frac{c^2 p}{\eta R^2 \varepsilon} \quad (23)$$

and using (12), (22) can be written as

$$\frac{d}{d\theta} \left[G \frac{d}{d\theta} (\bar{p} - \mu^* \theta (2\pi - \theta)) \right] = -12 \cos\theta, \quad (24)$$

where

$$G = \frac{-12(\psi_x - \beta\psi_z\sqrt{\theta(2\pi - \theta)})}{1 - \beta\sqrt{\theta(2\pi - \theta)}} + \frac{\bar{h}^3(4 + \bar{h}\bar{s}) + (\bar{s}\beta\gamma^*\bar{h}^2\sqrt{\theta(2\pi - \theta)})}{(1 + \bar{h}\bar{s})(1 - \beta\sqrt{\theta(2\pi - \theta)})}$$

Equation (24) is known as the non-dimensional form of Reynolds type equation.

IV. SOLUTION

Solving (24) under the pressure boundary conditions

$$\frac{d\bar{p}}{d\theta} = 0, \text{ when } \theta = \pi$$

and

$$\bar{p} = 0, \text{ when } \theta = 0, \tag{25}$$

one obtains the expression of non-dimensional film pressure \bar{p} as

$$\bar{p} = \mu^*(2\pi\theta - \theta^2) - 12 \int_0^\theta \frac{\sin\theta}{G} d\theta. \tag{26}$$

Now $W_x = LR \int_0^{2\pi} p \sin\theta d\theta$ and $W_z = LR \int_0^{2\pi} p \cos\theta d\theta$ are the components of load capacity in x and z -directions respectively, where L is the length of bearing. Here $W_x = 0$ as pressure is generated only in the direction of z -axis. Hence the average load carrying capacity $W = \sqrt{W_x^2 + W_z^2}$

is $W = W_z = LR \int_0^{2\pi} p \cos\theta d\theta$.

The non-dimensional form of W can be expressed as

$$\bar{W} = \frac{c^2 W}{\eta l R^3 \dot{\epsilon}} = 4\pi\mu^* + 12 \int_0^{2\pi} \frac{\sin^2\theta}{G} d\theta \tag{27}$$

V. RESULTS AND DISCUSSIONS

Using Simpson's one third Rule with step size $11/14$ and for water based magnetic fluid having density $\rho = 1400 \text{ kg/m}^3$ and viscosity $\eta = 0.012 \text{ kg/ms}$ and for fixed values of $c = 2.5 \times 0.00001$, $\bar{\mu} = 0.05$, $\eta_x = 0.81$, $\alpha^2 = 0.001$, $\epsilon = 0.3$, $\dot{\epsilon} = 0.02$, $\varphi_z = 10^{-10}$, $l = 0.002$, the length of bearing $L = 2\pi R = 0.05 \text{ m}$, the results for non-dimensional load carrying capacity (using (27)) are computed which are reflected in tables below. Moreover, when $K = 0$; FF effect without magnetic field and $K \neq 0$; FF effect with applied magnetic field. Similarly, $\alpha^2 = 0$; represents NR model and $\alpha^2 = 0.001$ represents JE model.

Many authors [12-15] concluded in their study that better performance is observed when Ferro-fluid is used as a lubricant in bearing systems in presence of applied magnetic field effect.

TABLE-1: \bar{W} in both models for various values of slip parameter s and magnetization parameter K

| $s \rightarrow$ | 5.56×10^4 | $5.56 \times 10^{4.5}$ | 5.56×10^5 | $5.56 \times 10^{5.5}$ | 5.56×10^6 | $K \downarrow$ |
|-----------------|--------------------|------------------------|--------------------|------------------------|--------------------|----------------|
| NR | 0.0025578 | 0.0246991 | 0.2494422 | 2.7605813 | 27.9920845 | 10^8 |
| JE | 0.2950114 | 0.2488331 | 0.2446306 | 0.2439117 | 0.2436991 | |
| NR | 0.0127441 | 0.0348853 | 0.2596284 | 2.7707675 | 28.0022717 | 10^{10} |
| JE | 0.2597015 | 0.2556163 | 0.2548245 | 0.2544377 | 0.2542568 | |
| NR | 1.0313665 | 1.0535077 | 1.2782509 | 3.7893898 | 29.0208931 | 10^{12} |
| JE | 1.2745618 | 1.2739044 | 1.2734478 | 1.2730941 | 1.2729164 | |
| NR | 102.8936081 | 102.9157486 | 103.1404953 | 105.6516342 | 130.8831329 | 10^{14} |
| JE | 103.1364365 | 103.136116 | 103.1356888 | 103.1353378 | 103.1351624 | |

- As shown in table-1, the data confirms that when the slip parameter $s < 5.56 \times 10^5$, the values of \bar{W} are better in the JE Model as compared to NR model. But when $s > 5.56 \times 10^5$, NR model should be preferred over JE model. Also in NR model, \bar{W} is increased with the increase of slip, but there is reverse trend in case of JE model.
- In both the models, increase in magnetization parameter K results in to increase in \bar{W} .
- It is clear from the table-1, that when we take the value of $K = 10^{12}$ and $K = 10^{14}$, there is high jump in the values of \bar{W} in both the models.

TABLE-2: \bar{W} for various values of porous thickness l and magnetization parameter K for fixed value of $s = 5.56 \times 10^5$

| $l \rightarrow$ $K \downarrow$ | 0.001 | 0.002 | 0.004 | 0.008 | 0.016 | Model Type |
|-----------------------------------|-----------|-----------|-----------|-----------|-----------|------------|
| 0 | 0.5067978 | 0.2493393 | 0.1236837 | 0.0615988 | 0.0307391 | NR |
| 10^8 | 0.5069007 | 0.2494422 | 0.1237865 | 0.0617017 | 0.030842 | |
| 10^{10} | 0.5170869 | 0.2596284 | 0.1339728 | 0.0718879 | 0.0410282 | |

| | | | | | | |
|-----------|------------|------------|------------|-------------|------------|----|
| 10^{12} | 1.5357094 | 1.2782509 | 1.1525953 | 1.0905104 | 1.0596507 | JE |
| 10^{14} | 103.397949 | 103.140495 | 103.014839 | 102.9527512 | 102.92189 | |
| 0 | 0.4873634 | 0.2446306 | 0.1225924 | 0.0614042 | 0.0307677 | |
| 10^8 | 0.4975799 | 0.2548245 | 0.1327806 | 0.071591 | 0.0409541 | |
| 10^{10} | 1.5162054 | 1.2734478 | 1.1514032 | 1.0902134 | 1.0595765 | |
| 10^{12} | 1.5162054 | 1.2734478 | 1.1514032 | 1.0902134 | 1.0595765 | |
| 10^{14} | 103.378449 | 103.135689 | 103.013649 | 102.9524536 | 102.921822 | |

As it is shown in table-2, for the fixed value of $s = 5.56 \times 10^5$, same scenario is found in both the models. i.e., the \bar{W} increase with the decrease in uniform porous thickness l . Moreover, the drastic change can be seen in \bar{W} when the magnetization parameter $K = 10^{14}$.

TABLE- 3: \bar{W} for various values of porous thickness l and slip parameter s for fixed value of magnetization parameter $K = 10^{12}$

| $s \rightarrow$ $l \downarrow$ | 5.56×10^4 | $5.56 \times 10^{4.5}$ | 5.56×10^5 | $5.56 \times 10^{5.5}$ | 5.56×10^6 | Model Type |
|-----------------------------------|--------------------|------------------------|--------------------|------------------------|--------------------|------------|
| 0.001 | 1.0338228 | 1.0782104 | 1.5357094 | 7.3940372 | 42.6111832 | NR |
| 0.002 | 1.0313665 | 1.0535077 | 1.2782509 | 3.7893898 | 29.0208931 | |
| 0.004 | 1.0301389 | 1.0411963 | 1.1525953 | 2.3271511 | 25.4978104 | |
| 0.008 | 1.0295252 | 1.0350506 | 1.0905104 | 1.6596582 | 8.9325218 | |
| 0.016 | 1.0292183 | 1.0319803 | 1.0596507 | 1.3399222 | 4.4691591 | |
| 0.001 | 1.5198261 | 1.5179479 | 1.5162054 | 1.5148108 | 1.5141087 | JE |
| 0.002 | 1.2745618 | 1.2739044 | 1.2734478 | 1.2730941 | 1.2729164 | |
| 0.004 | 1.151785 | 1.151527 | 1.1514032 | 1.1513135 | 1.1512687 | |
| 0.008 | 1.0903604 | 1.0902492 | 1.0902134 | 1.0901905 | 1.0901792 | |
| 0.016 | 1.059639 | 1.0595878 | 1.0595765 | 1.0595706 | 1.0595677 | |

From table-3, it is clear that when there is decrease in porous thickness, the value of W is increased in both the models. Also, when the value of slip parameters $< 5.56 \times 10^5$, JE model gives better results as compared to NR model and whens $> 5.56 \times 10^5$, NR model gives better results as compared to JE model.

TABLE-4: \bar{W} for various values of ϵ and magnetization parameter K for fixed value of $s = 5.56 \times 10^5$

| $\epsilon \rightarrow$ $K \downarrow$ | 0.2 | 0.02 | 0.002 | 0.0002 | Model Type |
|--|------------|-------------|--------------|---------------|------------|
| 0 | 0.2493393 | 0.2493393 | 0.2493393 | 0.2493393 | NR |
| 10^8 | 0.2493496 | 0.2494422 | 0.2503682 | 0.2596284 | |
| 10^{10} | 0.2503682 | 0.2596284 | 0.3522305 | 1.2782509 | |
| 10^{12} | 0.3522305 | 1.2782509 | 10.5384550 | 103.1404953 | |
| 10^{14} | 10.5384550 | 103.1404953 | 1029.1608887 | 10289.3652344 | |
| 0 | 0.2493393 | 0.2493393 | 0.2493393 | 0.2493393 | JE |
| 10^8 | 0.244538 | 0.2446306 | 0.2455566 | 0.2548168 | |
| 10^{10} | 0.2455643 | 0.2548245 | 0.3474265 | 1.2734469 | |
| 10^{12} | 0.3474273 | 1.2734478 | 10.5336514 | 103.1356888 | |
| 10^{14} | 10.5336514 | 103.1356888 | 1029.156128 | 10289.36035 | |

From table-4, it can be seen that when the value of ϵ decreases, the load carrying capacity increases in both models. However, when the value of K is more than 10^{12} , there is sudden high jump in load carrying capacity.

TABLE-5: \bar{W} for various values of ϵ and slip parameter s for fixed $K = 10^{12}$

| $s \rightarrow$ $\epsilon \downarrow$ | 5.56×10^4 | $5.56 \times 10^{4.5}$ | 5.56×10^5 | $5.56 \times 10^{5.5}$ | 5.56×10^6 | Model Type |
|--|--------------------|------------------------|--------------------|------------------------|--------------------|------------|
| 0.2 | 0.1053461 | 0.1274873 | 0.3522305 | 2.8633695 | 28.0948734 | NR |
| 0.02 | 1.0313665 | 1.0535077 | 1.2782509 | 3.7893898 | 29.0208931 | |
| 0.002 | 10.2915707 | 10.3137112 | 10.5384550 | 13.0495939 | 38.2810974 | |
| 0.0002 | 102.8936081 | 102.9157486 | 103.1404953 | 105.6516342 | 130.8831329 | |
| 0.2 | 0.3485414 | 0.3478841 | 0.3474273 | 0.3470736 | 0.346896 | JE |
| 0.02 | 1.2745618 | 1.2739044 | 1.2734478 | 1.2730941 | 1.2729164 | |
| 0.002 | 10.5347652 | 10.5341082 | 10.5336514 | 10.5332975 | 10.5331202 | |
| 0.0002 | 103.1368027 | 103.1361465 | 103.1356888 | 103.1353378 | 103.1351547 | |

Table-5 shows that when the value of slip parameter s increases, the load carrying capacity increases in case of NR model. But there is an opposite scenario in case of JE model. Moreover, when the value of ϵ is less than 0.002, there is sudden high jump in load carrying capacity in both the models.

TABLE-6: \bar{W} for various values of ϕ_z and magnetization parameter K for fixed value of $s = 5.56 \times 10^5$

| $\phi_z \rightarrow$ $K \downarrow$ | 10^{-8} | 10^{-9} | 10^{-10} | 10^{-11} | 10^{-12} | Model Type |
|--|-------------|-------------|-------------|-------------|-------------|------------|
| 0 | 0.2493393 | 0.2493393 | 0.2493393 | 0.2493393 | 0.2493393 | NR |
| 10^8 | 0.2494422 | 0.2494422 | 0.2494422 | 0.2494422 | 0.2494422 | |
| 10^{10} | 0.2596284 | 0.2596284 | 0.2596284 | 0.2596284 | 0.2596284 | |
| 10^{12} | 1.2782509 | 1.2782509 | 1.2782509 | 1.2782509 | 1.2782509 | |
| 10^{14} | 103.1404953 | 103.1404953 | 103.1404953 | 103.1404953 | 103.1404953 | |
| 0 | 0.2493393 | 0.2493393 | 0.2493393 | 0.2493393 | 0.2493393 | JE |
| 10^8 | 0.0025442 | 0.0245191 | 0.2446306 | 2.4824531 | 29.2859936 | |
| 10^{10} | 0.0127341 | 0.034739 | 0.2548245 | 2.4592919 | 24.8716373 | |
| 10^{12} | 1.0313569 | 1.0533649 | 1.2734478 | 3.4746382 | 25.5226669 | |
| 10^{14} | 102.8936005 | 102.9156036 | 103.1356888 | 105.3365555 | 127.348793 | |

Tabular values shown in table-6 confirms that change in ϕ_z does not affect the load carrying capacity in NR model, whereas the better load carrying capacity is obtained in case of JE Model according to increase in ϕ_z .

TABLE-7: \bar{W} for various values of ϕ_z and slip parameter s for fixed $K = 10^{12}$

| $s \rightarrow$ $\phi_z \downarrow$ | 5.56×10^4 | $5.56 \times 10^{4.5}$ | 5.56×10^5 | $5.56 \times 10^{5.5}$ | 5.56×10^6 | Model Type |
|--|--------------------|------------------------|--------------------|------------------------|--------------------|------------|
| 10^{-8} | 1.0313665 | 1.0535077 | 1.2782509 | 3.7893898 | 29.0208931 | NR |
| 10^{-9} | 1.0313665 | 1.0535077 | 1.2782509 | 3.7893898 | 29.0208931 | |
| 10^{-10} | 1.0313665 | 1.0535077 | 1.2782509 | 3.7893898 | 29.0208931 | |
| 10^{-11} | 1.0313665 | 1.0535077 | 1.2782509 | 3.7893898 | 29.0208931 | |
| 10^{-12} | 1.0313665 | 1.0535077 | 1.2782509 | 3.7893898 | 29.0208931 | |
| 10^{-8} | 1.031364 | 1.0313611 | 1.0313569 | 1.0313534 | 1.0313516 | JE |
| 10^{-9} | 1.0534393 | 1.0534072 | 1.0533649 | 1.0533298 | 1.0533121 | |
| 10^{-10} | 1.2745618 | 1.2739044 | 1.2734478 | 1.2730941 | 1.2729164 | |
| 10^{-11} | 3.5234149 | 3.4825563 | 3.4746382 | 3.4707692 | 3.4689603 | |
| 10^{-12} | 30.5694904 | 25.9436493 | 25.5226669 | 25.4507637 | 25.4294319 | |

Tabular values shown in table-7 confirms that in case of JE Model, when there is increase in values of ϕ_z , better \bar{W} is obtained. Also, in JE model, when the value of ϕ_z is more than or equal to 10^{-11} , the better load carrying capacity is obtained as compared to NR Model.

DISCUSSIONS ON POROUS STRUCTURES

The Globular Sphere Model (refer Fig. 5) proposed by Kozeny-Carman [19], in which the permeability of the assorted porous matrix is described as

$$k = \frac{D_c^2 \zeta^3}{180(1-\zeta)^2},$$

where D_c denotes the mean particle size and ζ denotes the porosity of the porous matrix.

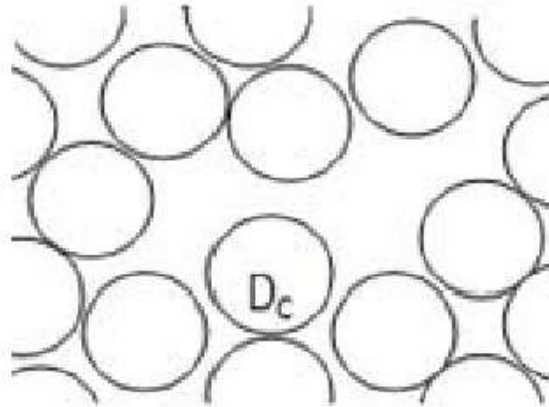


Fig. 4 Structure of Globular Sphere Model

Another Model namely capillary fissures model (refer Fig. 5) proposed by Irmay [19, 20], in which the permeability of the assorted porous matrix is described as

$$k = \frac{(1-m^2/3)D_s^2}{12m},$$

where D_s denotes the average diameter particle size and $m = 1 - \zeta$. Both the Models are well described in [22].

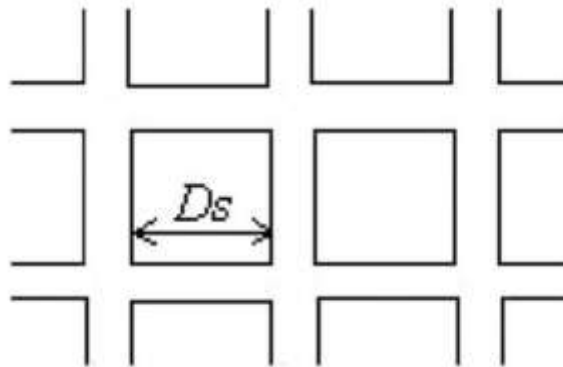


Fig. 5 Structure of Capillary Fissures Model

The following results and discussion are for the above discussed porous structures.

TABLE-8: \bar{W} for fixed value of $K = 10^{12}$ and $D_c = 0.001$ for Globular Sphere Model

| Flow Model | $\zeta = 0.1$ | $\zeta = 0.2$ | $\zeta = 0.3$ | $\zeta = 0.4$ | $\zeta = 0.5$ |
|------------|---------------|---------------|---------------|---------------|---------------|
| NR Model | 109.7494507 | 103.7930145 | 103.231987 | 103.085495 | 103.0340881 |
| JE Model | 108.3157425 | 103.7501068 | 103.2237778 | 103.0822296 | 103.0320587 |

As per the tabulated values in Table-8, it is clear that for fixed $K = 10^{12}$ and $D_c = 0.001$, better \bar{W} is obtained when ζ decreases.

TABLE-9: \bar{W} for fixed value of of $K = 10^{12}$ and $D_s = 0.001$ for Capillary fissures Model

| Flow Model | $\zeta = 0.1$ | $\zeta = 0.2$ | $\zeta = 0.3$ | $\zeta = 0.4$ | $\zeta = 0.5$ |
|------------|---------------|---------------|---------------|---------------|---------------|
| NR Model | 102.8959808 | 102.8938141 | 102.8931427 | 102.8928528 | 102.892746 |
| JE Model | 102.8959732 | 102.8938141 | 102.8931427 | 102.8928528 | 102.892746 |

Tabular values in Table-9 confirms that for fixed $K = 10^{12}$ and $D_s = 0.001$, there is no much change in \bar{W} is observed with the change in ζ . Also, in comparison point of view, better \bar{W} is obtained in case of the Globular Sphere Model rather than the Capillary fissures Model (from Table-8 and Table-9).

TABLE-10: \bar{W} for fixed value of of $K = 10^{12}$ and $\zeta = 0.1$ for Globular Sphere Model

| Flow Model | $D_c = 0.1$ | $D_c = 0.01$ | $D_c = 0.001$ |
|------------|-------------|--------------|---------------|
| NR Model | 102.8917007 | 102.9459152 | 109.7494507 |
| JE Model | 102.8917007 | 102.9455566 | 108.3157425 |

As per the results shown in Table-10 one can see that, \bar{W} increases with decrease in D_c . Also, one can observe sudden increase in \bar{W} after $D_c = 0.01$ for Globular Sphere Model.

TABLE-11: \bar{W} for fixed value of of $K = 10^{12}$ and $\zeta = 0.1$ for Capillary fissures Model

| Flow Model | $D_s = 0.1$ | $D_s = 0.01$ | $D_s = 0.001$ |
|------------|-------------|--------------|---------------|
| NR Model | 102.8917007 | 102.9459152 | 102.8959808 |
| JE Model | 102.8911514 | 102.8912048 | 102.8959732 |

As per the Table-11 results it is clear that, no much change in \bar{W} observed as decrease in D_s when Capillary fissures Model is considered. Also, from Table-10 and Table-11, one can observe that for very small size of solid particles gives better performance when the Globular Sphere Model is considered as compared to Capillary fissures Model.

VI. CONCLUSIONS

The present study deliberates NR model and JE model for magnetic fluid flow by aspect of hydrodynamic theory of lubrication for axially undefined porous journal bearing having porous attached on the outer surface of journal. The results of non-dimensional load carrying capacity are shown for various parameters like slip velocity, porous thickness, squeeze velocity, eccentricity, permeability in tables. Based on the results and discussions, the following conclusions can be made:

- In case of NR model, better \bar{W} is obtained as soon as the value of slip starts with 5.56×10^5 .
- \bar{W} is much better in both the models once magnetic field parameter K is more than 10^{12} .
- \bar{W} is better observed in case of the uniform porous layer thickness l is smaller.
- \bar{W} is better obtained when squeeze velocity $\dot{\epsilon}$ is decreased in both the models and it is observed that when $\dot{\epsilon} = 0.002$, \bar{W} is rapidly increased.
- Increase in φ_z results increase in \bar{W} in case of JE model and to get better \bar{W} , one should choose $\varphi_z \geq 10^{-11}$.

In the presence of applied (variable) external magnetic field (having magnetic field parameter $K \geq 10^{12}$), this study concludes that, to design a magnetic fluid lubricated axially undefined porous journal bearing with porous layer of smaller thickness attached on journal having smallest amount of squeeze velocity, NR model is more preferable over JE model with $s = 5.56 \times 10^5$ or more. If one wants to consider the JE model to design such bearing, the values of parameters should be taken in to consideration. Moreover, the Globular Sphere Model is more suitable than the Capillary fissures Model for porous structure.

VII. REFERENCES

- [1] G. A. Maugin, The Method of Virtual Power in Continuum Mechanics: Application to Coupled Fields, Acta Mathematica Vol. 35 I, 1980, pp. 1-70.
- [2] V.T. Morgan, A. Cameron, Mechanism of lubrication in porous metal bearings, Conference on Lubrication and Wear, Paper 89, London, 1957.
- [3] J. L. Neuringer and R. E. Rosensweig, "Magnetic fluids," The Physics of Fluids, vol. 7, no. 12, 1964, pp. 1927–1937. DOI:10.1017/s0022112089220773
- [4] J. T. Jenkins, "A theory of magnetic fluids," Archive for Rational Mechanics and Analysis, vol. 46, 1972, pp. 42–60.
- [5] B. L. Prajapati, On certain theoretical studies in hydrodynamic and electro-magneto hydrodynamic lubrication [Ph.D. thesis], S.P. University, Vallabh Vidhyanagar, India, 1995.
- [6] M. V. Bhat, Lubrication with a Magnetic Fluid, Team Spirit India, Ahmedabad, India, 2003.
- [7] P. Ram and P. D. S. Verma, "Ferrofluid lubrication in porous inclined slider bearing," Indian Journal of Pure and Applied Mathematics, vol. 30, no. 12, 1999, pp. 1273–1281.
- [8] R. C. Shah, D. B. Patel, Mathematical Modeling of newly Designed Ferrofluid Based Slider Bearing Including Effects of Porosity, Anisotropic Permeability, Slip Velocity at both the Ends, and Squeeze Velocity, Applied Mathematics, Vol. 2(5): 2012, pp. 176-183.
- [9] V.K. Agrawal, Magnetic fluid based porous inclined slider bearing, Wear Vol. 107, 1986, pp. 133–139. DOI:10.1016/0043-1648(86)90023-2
- [10] J. Prakash and S.K. Vij, Hydrodynamic lubrication of a porous slider, J. Mech. Engg. Sci. Vol. 15, 1973, pp. 232–234. DOI:10.1243/jmes_jour_1973_015_039_02.
- [11] G.S. Beavers and D.D. Joseph, Boundary conditions at a naturally permeable wall, J. Fluid. Mech. Vol. 30, 1967, pp. 197–207. DOI: 10.1017/s0022112067001375
- [12] R. C. Shah and D. B. Patel, Squeeze Film Based on Ferrofluid in Curved Porous Circular Plates with Various Porous Structure, Appl. Math., Vol. 2, 2012, pp. 121–123.
- [13] R. C. Shah and N. I. Patel, Impact of various and arbitrary porous structure in the study of squeeze step bearing lubricated with magnetic fluid considering variable magnetic field, Proc IMechE Part J: J Engineering Tribology, 2014, pp. 1–14.
- [14] D. A. Patel, M. Joshi and D. B. Patel, Design of porous step bearing by considering different Ferro Fluid lubrication flow models. Journal of Manufacturing Engineering, Vol. 16(4), 2021, pp. 108-114.
- [15] D. A. Patel, M. Attri and D. B. Patel, Performance of Hydrodynamic Porous Slider Bearing with Water based Magnetic Fluid as a

- Lubricant: Effect of Slip and Squeeze Velocity, Journal of Scientific and Industrial Research (JSIR), Vol. 80 (6), 2021, pp. 508-512.
- [16] S.Soni and D. P. Vakharia, Performance Analysis of Short Journal Bearing under Thin Film Lubrication. ISRN Mechanical Engineering, 2014, pp. 1–8.DOI:10.1155/2014/281021
- [17] R. M. Mane and S. Soni, Analysis of hydrodynamic plain journal bearing, Proceedings of the COMSOL Conference, Bangalore, India 2013.
- [18] R. C. Shah and D. B. Patel, Mathematical analysis of newly designed ferrofluid lubricated double porous layered axially undefined journal bearing with anisotropic permeability, slip velocity and squeeze velocity, International Journal of Fluid Mechanics Research, Vol. 40 (5), 2013, pp. 446-454. DOI: 10.1615/InterJFluidMechRes.v40.i5.70
- [19] Liu J. Analysis of a porous elastic sheet damper with a magnetic fluid. Journal of Tribology, 131, 2009, pp. 0218011-15.
- [20] S. Irmay, Flow of liquid through cracked media. Bull. Res. Council Isr., Vol. 5A(1): 84, 1955.
- [21] E.M. Sparrow, G.S. Beavers and I.T. Hwang, Effect of velocity slip on porous walled squeeze films, J. Lubr. Technol. Vol. 94, 1972, pp. 260–265..DOI:10.1115/1.3451704
- [22] Shah RC and Patel NI, Impact of various and arbitrary porous structure in the study of squeeze step bearing lubricated with magnetic fluid considering variable magnetic field, Proc IMechE Part J:EngineeringTribology, 0(0), 2014, pp. 1-14

AUTHOR PROFILE

Dipak A Patel



is working as an Assistant Professor, Humanities and Sciences Department, Government Engineering College Palanpur – 385001, Gujarat State, India. He has more than 14 years of teaching experience. His area of specialization includes Mathematical Modelling, Fluid Dynamics. He has published 4 publications in International Journals/Conferences.

Manisha Joshi



is working as a Dean, Undergraduate Program, IILM University, Gurugram – 122003, Haryana, India. She has more than 15 years of teaching experience. Her area of specialization includes Mathematical optimisation problems, Modelling in Fuzzy Environment, Quantitative Methods, Fractals, Non- linear dynamics. She has 8 publications.

Dilip B. Patel



is working as an Assistant Professor, Department of Basic Sciences and Humanities, College of Renewable Energy and Environmental Engineering, Sardar-Krushinagar Dantiwada Agricultural University, Sardarkrushinagar – 385506, Gujarat State, India. He has more than 17 years of teaching experience. His area of specialization includes Mathematical Modelling, Fluid Dynamics. He has published 25 publications in International and National Journals/Conferences.